**TECHNICAL PAPER**

# In Situ Experimental Study of Carbon Monoxide Generation by Gasoline-Powered Electric Generator in an Enclosed Space

**Liangzhu Wang, Steven J. Emmerich, and Andrew K. Persily**
*Indoor Air Quality and Ventilation Group, Building Environment Division, Building and Fire Research Laboratory, National Institute of Standards and Technology, Gaithersburg, MD*

## ABSTRACT

On the basis of currently available data, approximately 97% of generator-related carbon monoxide (CO) fatalities are caused by operating currently marketed, carbureted spark-ignited gasoline-powered generators (not equipped with emission controls) in enclosed spaces. To better understand and to reduce the occurrence of these fatalities, research is needed to quantify CO generation rates, develop and test CO emission control devices, and evaluate CO transport and exposure when operating a generator in an enclosed space. As a first step in these efforts, this paper presents measured CO generation rates from a generator without any emission control devices operating in an enclosed space under real weather conditions. This study expands on previously published information from the U.S. Consumer Product Safety Commission. Thirteen separate tests were conducted under different weather conditions at half and full generator load settings. It was found that the CO level in the shed reached a maximum value of $29,300 \pm 580$ mg/m$^3$, whereas the oxygen (O$_2$) was depleted to a minimum level of $16.2 \pm 0.02\%$ by volume. For the test conditions of real weather and generator operation, the CO generation and the O$_2$ consumption could be expressed as time-averaged generation/consumption rates. It was also found that the CO generation and O$_2$ consumption rates can be correlated to the O$_2$ levels in the space and the actual load output from the generator. These correlations are shown to agree well with the measurements.

## IMPLICATIONS

Operating a gasoline-powered electric generator indoors or in an attached space (e.g., a garage) can cause CO levels in the occupied space to reach a potentially lethal level within a short period of time. Reducing these exposures involves many steps, including achieving a better understanding of the CO generation rates from these devices under typical operating conditions. This paper presents a methodology for measuring these emission rates under more realistic conditions than a laboratory chamber or an engine test stand. The rates obtained and the methodology will provide a basis for subsequent research on approaches to reducing generator emissions rates of CO as well as studies of CO transport from attached spaces into occupied portions of buildings.

## INTRODUCTION

During the years 1999–2007, there were 474 deaths known to be caused by carbon monoxide (CO) poisoning associated with the use of engine-driven tools in U.S. households, and 85% of these fatalities were associated with gasoline-powered electric generators not equipped with emission control technology.[1] Ninety-seven percent of the 327 generator-related CO fatalities, which included generator location information, were associated with operating these carbureted generators in enclosed spaces (e.g., a basement, garage, shed, or crawl space) on the basis of investigations by the U.S. Consumer Product Safety Commission (CPSC).[1] These CO poisoning accidents often occurred after severe weather events (e.g., hurricanes, tornadoes, floods, ice storms, and blizzards) when generators were used to provide electrical power. From 1999 to 2007, approximately one third of all generator-related CO deaths were associated with power outages, 36% of which occurred during hurricanes in the Gulf States and snow storms in the Midwest and Carolinas in 2005.[1] Because the possession of household generators in the United States has climbed continuously in recent years, from an estimated 9.2 million units in 2002 to 10.6 million units in 2005, it is important to avoid future generator-related CO poisoning incidents, especially those associated with operating a generator indoors.[2] Measures have been taken to educate people not to operate generators indoors and to require manufacturers of portable generators to warn consumers of CO hazards through a warning label.[3] Nevertheless, the emission characteristics of these generators needs to be better understood. To establish a baseline CO emission rate of current generators, an experimental research effort was conducted of CO generation rates associated with generator operation in enclosed spaces and their effect on residential CO exposure. As part of this overall effort, CO emission control devices for generators are also being investigated. The paper presented here constitutes a first step in these efforts; that is, to quantify the baseline CO generation rate for generators operated indoors.

The initial health impact of CO is caused by anoxia, or deprivation of oxygen supply. When inhaled, CO preferentially binds with the oxygen carrier in erythrocytes, hemoglobin (Hb), to form carboxyhemoglobin (COHb), which causes the anoxia.[4] Indoor sources of CO are virtually always fuel-burning devices, such as a gasoline-powered engine.[5] Gasoline-engine-related CO

generation has mostly been studied in relation to the control of tailpipe emissions from automobiles, in which an engine usually runs under ambient air conditions during testing.[6] Kern et al.[7] studied oxygen ($O_2$) consumption and CO generation from an idling car in an enclosed garage and found that the CO generation rate was significantly higher than when running the car outside. Not many studies have been conducted directly on CO generation and $O_2$ consumption associated with gasoline-powered generators running indoors. Brown[8] studied the CO generation from four different commercially available generators in an enclosed experimental chamber, where air temperature and air change rate were controlled to provide different operating conditions, although the air change rates were generally quite high compared with typical residences. Steady-state CO concentrations were found to be more than 7400 parts per million by volume (ppmv), and $O_2$ levels were as low as 18.5%.[8] CO generation and $O_2$ consumption rates at steady state were also calculated and were found to be affected by $O_2$ level, generator loading, and/or chamber air temperature.

However, a generator operating in an enclosed space such as a garage or a storage shed, as opposed to a laboratory chamber, will be subject to uncontrolled temperatures and to lower ventilation rates determined by ambient weather conditions. Moreover, the CO levels under actual operation are actually a transient process, and CO could reach levels of concern far before steady state is achieved. To study generator CO emissions under more realistic conditions, tests were conducted in a single-zone space in part to support the development of CO emission control devices. This paper reports on the first step in these efforts to quantify CO generation rates from generators without emission controls in a nonlaboratory facility. To determine generator CO generation, a single-zone space is adequate for this phase of the study and simpler when compared with a multispace case, in which interzonal airflows and CO transport may occur and are often hard to be measured. Correlations to predict CO generation and $O_2$ consumption under transient operation were developed. The experimental methods and prediction models in this paper also provide the fundamentals for future phases of this research effort. The CO generation rates will be used as the baseline for the evaluations of emission control devices. In addition, the correlations developed in this paper will also be used for the prediction of CO migration and exposure in multispace residential houses.

## THEORY AND METHOD

To model a generator running inside of an enclosed single-zone space, a theoretical model was constructed based on Figure 1. Assuming a gas component, $C$, is either generated ($S_C > 0$) or consumed ($S_C < 0$) in the zone, a differential mass balance equation for $C$ during a period of $\Delta t = t_2 - t_1$ can be obtained

$$\rho_{C,in} V_s \frac{dC}{dt} = S_C - \rho_{C,in} C Q_{out} + \rho_{C,out} C_{out} Q_{in} \tag{1}$$
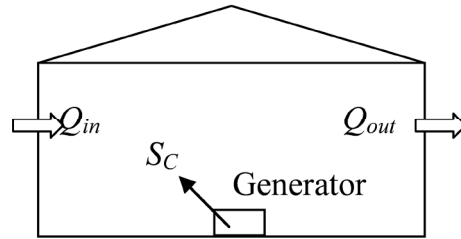


**Figure 1.** Schematic of a generator operating in a single-zone space.

by assuming
- The gas component, $C$, is an ideal gas
- The concentration of $C$ is uniform in the zone
- $\rho_C$, $S_c$, and $Q$ are constant during $\Delta t$
- The mass of fuel added from the generator to the zone air is neglected

The density of $C$ in eq 1 can be obtained by the ideal gas law. $S_C$ is positive when referred to as $S_{CO}$ (the generation rate of CO) and negative for $S_{O2}$ (the consumption rate of $O_2$). In the experiments presented in this paper, the concentration of a gas component, $C$, was measured by a gas analyzer, as described below. The air change rate, $Q$, was determined using the tracer gas decay method using sulfur hexafluoride ($SF_6$). Given that $SF_6$ may decompose at temperatures above 200 °C,[9] the potential consumption of $SF_6$ in the generator engine, $S_{SF6}$ ($<0$), was examined. For $SF_6$, $C_{SF6,out} = 0$. Assuming a pulse of $SF_6$ is injected into a space during a time period of $\Delta t$, the mass balance of $SF_6$ is expressed as follows:

$$\frac{dC_{SF6}}{dt} = \frac{S_{SF6}}{\rho_{SF6,in} V_s} - C_{SF6} A_{out} \tag{2}$$

The decomposition of $SF_6$ in the generator can be calculated as

$$S_{SF6} = \rho_{SF6,in} K_{SF6,d} C_{SF6} Q_{gen,in} \tag{3}$$

where $K_{SF6,d}$, the $SF_6$ decomposition ratio is determined by

$$K_{SF6,d} = \frac{C_{SF6,ex} - C_{SF6,in}}{C_{SF6,in}} \leq 0 \tag{4}$$

$K_{SF6,d}$ can be obtained by comparing $SF_6$ concentrations at the generator engine air intake and exhaust. $K_{SF6,d}$ was found to be approximately $-4\%$ from the tests on $SF_6$ decomposition.

Solving eq 2 for $SF_6$ during $\Delta t = t_2 - t_1$,

$$A_{out} = \frac{(\ln C_{SF6,t1} - \ln C_{SF6,t2})}{t_2 - t_1} + \frac{K_{SF6,d} Q_{gen,in}}{V_s} \tag{5}$$

The second term at the right-hand side shows the effect of any $SF_6$ decomposition on the air change rate, and the first term is determined by the $SF_6$ decay method.[10] When the generator operates at the peak rotational speed of 3750 min$^{-1}$, the second term in eq 5 is approximately

$-0.03$ hr$^{-1}$, much less than the air change rates of the shed in the tests, which are typically in the range of 0.7–7.6 hr$^{-1}$. Therefore, the effect of SF$_6$ decomposition on the air change rate measurement was insignificant in this study.

For a four-stroke engine, which is common for generators, the airflow through the engine, $Q_{gen,in}$, can be calculated.[11]

$$Q_{gen,in} = \eta_{gen} D_{gen} \frac{RPM}{2} \qquad (6)$$

For a typical gasoline engine, the volumetric efficiency ($\eta_{gen}$) ranges from 80 to 90%.[11] For example, when $\eta_{gen}$ is 85% and the generator in this study operates at 3750 min$^{-1}$, the displacement ($D_{gen}$) = 305 × 10$^{-6}$ m$^3$. The calculated $Q_{gen,in}$ is then 29.2 ± 2 m$^3$/hr.

After determining the air change rate of the space, $S_{CO}$ and $S_{O2}$ can be solved from eq 1 for the time period of $t_1$ to $t_2$.

$$S_{CO} = \rho_{CO,in} A_{out} V_s \frac{C_{CO,t2} - C_{CO,t1} e^{-A_{out}\Delta t}}{1 - e^{-A_{out}\Delta t}} \qquad (7)$$

$$S_{O2} = \rho_{O2,in} A_{out} V_s \frac{C_{O2,t2} - C_{O2,t1} e^{-A_{out}\Delta t}}{1 - e^{-A_{out}\Delta t}} - \frac{\rho_{O2,out} A_{out} V_s}{K_{m,\rho}} C_{O2,out} \qquad (8)$$
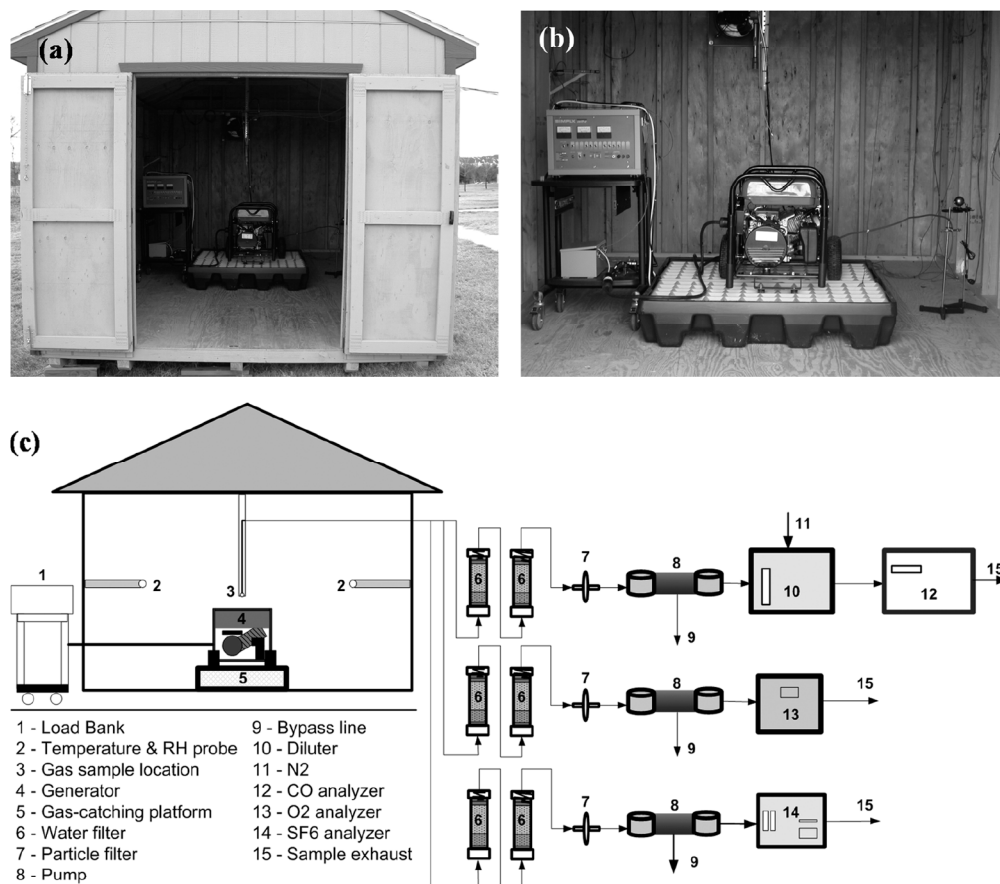
## EXPERIMENTAL SETUP

The experiments were conducted in a single-zone shed with dimensions of 4.88 m (length) × 3.05 m (width) × 2.90 m (height) as shown in Figure 2. The same carbureted generator as reported on by Brown[8] was placed on a gasoline-catching platform in the middle of the shed. The generator has a full-load power rating of 5.5 kW (~40% of portable generators are in the 5- to <6.5-kW power output range[2]). A portable AC load bank was used to draw electrical power. Generator loading can be manually selected with a maximum value of 10 kW in steps of 250 W. The load bank was located outside of the shed during a test as seen in Figure 2c. An explosion-proof exhaust fan was installed at the opposite wall to the door for shed ventilation at the end of a test and for quick exhaust during an emergency. The shed also had two operable windows at both sidewalls, which could be adjusted to vary the air change rate.

Separate sample lines were placed mid-height in the center of the shed (midway between the walls) for CO, O$_2$, and SF$_6$. A nondispersive infrared CO analyzer, a portable O$_2$ analyzer, and a gas chromatograph with an electron capture detector were used to measure CO, O$_2$, and SF$_6$, respectively. A gas divider/diluter was also used to dilute the sampled CO for the CO analyzer. To protect the analyzers from condensed water and/or soot particles, water desiccant and high-efficiency particulate air filters were used in the sampling system. The air temperature and

1 - Load Bank
2 - Temperature & RH probe
3 - Gas sample location
4 - Generator
5 - Gas-catching platform
6 - Water filter
7 - Particle filter
8 - Pump
9 - Bypass line
10 - Diluter
11 - N2
12 - CO analyzer
13 - O2 analyzer
14 - SF6 analyzer
15 - Sample exhaust

**Figure 2.** (a) Front and (b) inside views of the test shed and (c) schematic of experimental setup.

humidity in the shed were measured at two locations near two sidewalls. The air change rate was measured using a tracer gas decay method.[10] A pulse of $SF_6$ was injected for approximately 2–3 min at a central location in the shed, approximately three quarters up from the shed floor to the ceiling. All concentration, air temperature, and humidity data were recorded by an automated data acquisition system.

To validate the test setup, a series of preliminary tests were conducted. These included several gas concentration uniformity tests that were conducted by collecting samples at five different locations in the shed. It was found that the thermal plume, which was driven by the heat from the running generator, mixed the shed very well throughout testing. The variations among the five sample locations were less than 5% for $SF_6$, which met the uniformity requirement of 10% in the American Society for Testing and Materials standard for determining air change in a single zone.[10] Another series of tests were also conducted to determine the potential decomposition ratio of $SF_6$ in the generator engine, $K_{SF6,d}$ in eq 4. As described previously, the average $K_{SF6,d}$ from the preliminary tests was approximately 4%. Because $K_{SF6,d}$ is related to air and fuel flow rates through a combustion engine, combustion flame temperature, and engine mixing condition,[12] the value could vary among the tests.

## RESULTS AND DISCUSSIONS

Using the same generator in small chamber tests, Brown[8] found that CO generation rate was closely related to generator load and $O_2$ level. In this study, 13 tests were conducted for load settings of 2.5 kW (half of the maximum load of the generator) and 5 kW (full load) for different air change rates (which result in different $O_2$ levels) and air temperature as shown in Table 1. Different air change rates were achieved by adjusting the shed windows to be opened with a 0.05- by 0.2-m crack (OW = opened window) or completely closed (= closed window). Each test was also conducted at least twice to confirm the validity of the measurement data. Each test in Table 1 was named by its load setting, window adjustment, and repeat times; for example, 2.5kW-OW-1 indicates the first test running under a 2.5-kW load setting and with open windows. Note that tests 6, 11, and 12 were conducted after

the generator engine was serviced (S = serviced). For test 13, the shed was tightened to achieve a low air change rate (LA = lower air change rate).

### Levels of CO and $O_2$

Table 1 shows that there were large variations of CO and $O_2$ levels between tests with the generator operating at half- or full-load settings, and with the shed windows closed or opened. The CO level reached only 3700 mg/m$^3$ within 80 min in test 1 when the generator was half-loaded with the shed windows opened but reached a maximum of 29,300 mg/m$^3$ for an 86-min run time for a fully loaded generator in test 13 when the shed was tightened. The shed $O_2$ concentration dropped significantly when operating the generator in this enclosed space. The largest decline occurred for test 13, when the $O_2$ level was 16.2% with the low air change rate and fully loaded generator. Table 1 provides measured air change rates and Table 2 time-averaged weather conditions. When the shed was tightened in test 13, the air change rate reached its lowest value, 0.7 hr$^{-1}$, which explains its having the highest CO level and largest $O_2$ depletion. For the rest of tests, the shed window positions played an important role. The air change rates of open-window cases were all as high as or higher than those of closed windows. As a result, the opened window tests always had higher $O_2$ than those with closed windows for the same load. The CO levels in opened-window tests were generally lower than closed-window cases. It was then clear that the effect of air change rate on CO levels was directly related to $O_2$ level. Note also that the weather conditions during these tests varied significantly. The ambient temperature ranged from 4 °C to 17.2 °C, wind speed from 1.1 to 6.8 m/sec, and wind direction from 29° to 318° relative to the north. The variations of weather provided realistic generator operating conditions for these experiments compared with the controlled chamber experiments of previous studies.

As noted, the $O_2$ concentration had a major impact on CO level, as shown by Figure 3, which compares test 1 with test 13, the latter test having the lowest air change rate. The patterns of CO concentrations in both tests were almost an inverse to that of the $O_2$ level. The CO level was low at the beginning of generator startup and increased

**Table 1.** Test summaries of measured CO/$O_2$ concentrations, air change rates, and selected 5-min averaged CO generation and $O_2$ consumption rates.

| Load Setting (kW) | Test | Name | Run Time (min) | Maximum CO mg/m$^3$ (ppmv) | Minimum $O_2$ (%) | CO Generation Range (g/hr) | $O_2$ Consumption Range (g/hr) | Air Change Rate (hr$^{-1}$) |
|---|---|---|---|---|---|---|---|---|
| 2.5 | 1 | 2.5kW-OW-1 | 80 | 3,700 (3,190) | 19.3 | 340–900 | 3,300–4,800 | 6.5 |
| | 2 | 2.5kW-OW-2 | 63 | 6,100 (5,290) | 18.9 | 40–900 | 3,300–4,000 | 3.7 |
| | 3 | 2.5kW-CW-1 | 86 | 27,500 (23,950) | 16.9 | 1,100–3,100 | 4,600–5,900 | 2.6 |
| | 4 | 2.5kW-CW-2 | 101 | 26,800 (23,270) | 16.8 | 1,000–3,000 | 4,200–5,700 | 3.1 |
| | 5 | 2.5kW-CW-3 | 80 | 23,100 (20,090) | 17.1 | 880–2,600 | 4,100–5,100 | 2.9 |
| | 6 | 2.5kW-CW-S1 | 106 | 9,400 (8,160) | 18.2 | 500–1,400 | 4,200–5,100 | 3.6 |
| 5.0 | 7 | 5.0kW-OW-1 | 90 | 20,900 (18,210) | 17.9 | 120–3,700 | 5,700–7,100 | 4.7 |
| | 8 | 5.0kW-OW-2 | 81 | 9,700 (8,420) | 19.1 | 1,500–2,600 | 4,100–6,500 | 7.6 |
| | 9 | 5.0kW-CW-1 | 62 | 24,500 (21,320) | 17.4 | 1,100–3,600 | 5,600–6,700 | 3.7 |
| | 10 | 5.0kW-CW-2 | 74 | 24,400 (21,200) | 17.1 | 1,700–3,000 | 4,700–6,400 | 2.9 |
| | 11 | 5.0kW-CW-S1 | 65 | 25,800 (22,470) | 16.9 | 1,600–3,500 | 5,800–7,600 | 3.0 |
| | 12 | 5.0kW-CW-S2 | 66 | 25,600 (22,280) | 17.0 | 70–3,800 | 1,400–7,100 | 3.6 |
| | 13 | 5.0kW-CW-LA | 86 | 29,300 (25,500) | 16.2 | 2,000–3,400 | 3,900–6,200 | 0.7 |

**Table 2.** Ambient conditions and measured shed air temperatures for different leakage conditions.

| Test | Average Ambient Temperature (°C) | Avg. Wind Velocity (m/sec) | Average Wind Direction (°relative to north) | Shed Temperatures (°C) | Leakage Conditions |
|---|---|---|---|---|---|
| 1 | 15.1 | 4.0 | 198 | 21–50 | Open window |
| 2 | 5.4 | 1.2 | 56 | 11–39 | Open window |
| 3 | 15.6 | 1.1 | 279 | 32–50 | Closed window |
| 4 | 17.2 | 2.1 | 175 | 30–53 | Closed window |
| 5 | 13.8 | 1.3 | 245 | 32–52 | Closed window |
| 6 | 4.0 | 2.3 | 194 | 15–43 | Closed window |
| 7 | 7.1 | 1.8 | 262 | 12–52 | Open window |
| 8 | 5.3 | 6.8 | 314 | 17–39 | Open window |
| 9 | 7.9 | 3.6 | 318 | 12–44 | Closed window |
| 10 | 13.7 | 2.2 | 281 | 24–51 | Closed window |
| 11 | 8.1 | 3.1 | 29 | 17–41 | Closed window |
| 12 | 8.6 | 2.3 | 164 | 24–45 | Closed window |
| 13 | 5.7 | 1.6 | 218 | 12–39 | Tightened shed |

steadily with the drop of $O_2$. When $O_2$ dropped further and caused a very rich fuel mixture in the engine, CO reached a maximum level. Test 13 in Figure 3 shows an extreme case in which the generator eventually produced a zero electrical load when the $O_2$ dropped to approximately 16.4%, although it was set at a full load and the piston was still moving.

Figure 3 also shows that a complete steady state was never reached for both tests. A relatively stable period occurred at approximately 40 min for test 1 and 45 min for test 13 but only held for a few minutes. These results differed from the chamber experiments, in which CO concentrations became constant after a period of time and a complete steady state could be achieved under the controlled environment and higher air change rate.[8] Although these chambers tests are useful for some purposes, these results from the shed confirm the importance of studying CO generation as a transient process under real weather conditions and more realistic air change rates to better understand performance in the field.

### CO Generation and $O_2$ Consumption Rates
To generalize these test results to other conditions beyond this particular test facility, it is important to convert the results into CO generation and $O_2$ consumption rates. As seen in these tests, many factors directly or indirectly affected these rates, including space ventilation condition, combustion conditions in the engine, $O_2$ level in the space, load setting, and the time over which the generator has been running. Therefore, it is important to relate these parameters to the generation of CO and consumption of $O_2$.

Figure 4, a and b, illustrate how 5-min average CO generation rates and $O_2$ consumption rates ($\Delta t = 5$ min in eqs 7 and 8) change with $O_2$ levels in the 13 tests. Figure 4a shows that for full- and half-load settings, CO generation rates increased with decreasing $O_2$, reached maximum values when $O_2$ dropped to certain levels, and then declined further at even lower $O_2$ levels. This is consistent with the previous observation in Figure 3 that CO concentration leveled out at a certain $O_2$ level and dropped later for a richer fuel mixture. Under the extreme case of test 13, the CO rate decreased dramatically as the $O_2$ level reached approximately 16.4% with an electrical output of zero. Figure 4b shows an opposite trend of $O_2$ consumption rate compared with CO. The $O_2$ consumption rate decreased notably near 16.4%, corresponding to the previous explanation of the zero electrical output caused by
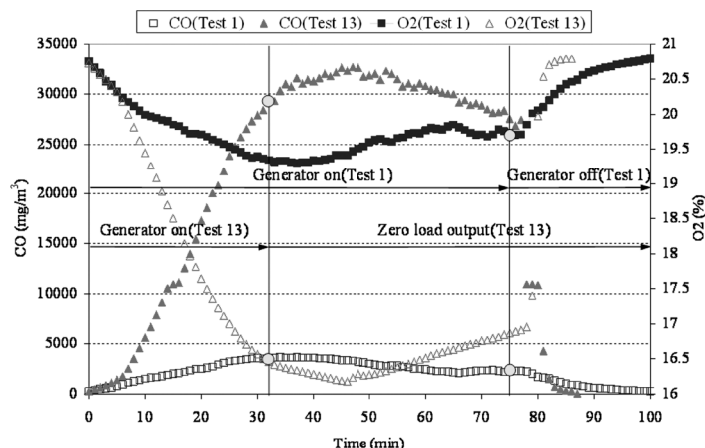


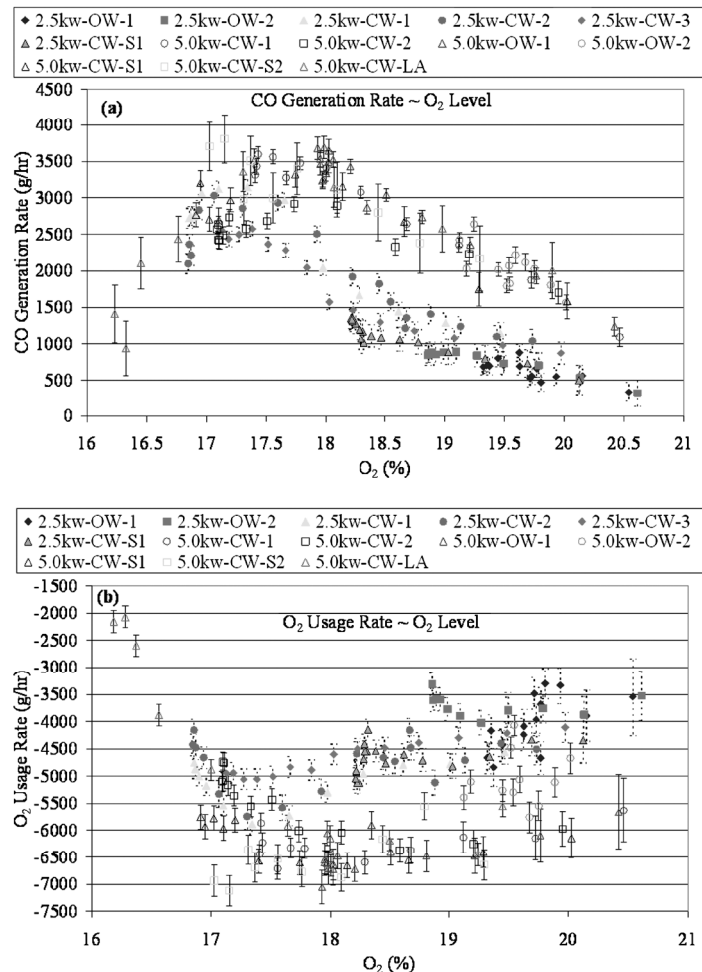**Figure 3.** Measured CO and $O_2$ concentrations of tests 1 and 13.

**Figure 4.** Five-minute averaged (a) CO generation rates and (b) $O_2$ consumption rates at different $O_2$ levels.

$O_2$ deficiency. Given that the engine piston was still moving, the $O_2$ consumption rate was not quite zero, which explains the continual drop of $O_2$ in test 13 of Figure 3, although the electrical output was zero.

The solid points in Figure 4 are data points for a half-load setting (2.5 kW) and the hollow ones are for a full-load setting (5 kW). As expected, a higher load setting generally results in more CO generated and $O_2$ consumed until the $O_2$ level reaches approximately 17%, where lines of full and half loads intersect. This intersection corresponds to the drop in electrical output with the decrease of $O_2$. Note that Figure 4 also shows the calculated uncertainty for each data point of CO generation and $O_2$ consumption rates, which was mostly less than 20% with a confidence level of 95%. The appendix to this paper discusses the uncertainty analysis in detail.

Figure 5 shows that the generator could sustain the electric load during most of the time for a half-load setting (e.g., in test 6), whereas it failed to provide full power for a full-load setting in the rest of the cases. When $O_2$ dropped to 17%, the real load output was only 2.5 kW, although the load setting was 5 kW. The rates of CO generation and $O_2$ consumption were therefore related to the actual electrical output rather than the load setting.

## Characterization of CO Generation and $O_2$ Consumption Rates

As discussed earlier, the rates of CO generation and $O_2$ consumption are potentially functions of multiple parameters, such as shed $CO/O_2$ levels, actual electrical output, air change rate, air temperature and humidity, and volume of the enclosed space. Excluding the time dependence by using time-average values, this dependence can be expressed as follows:

$$S_{CO} = f(C_{CO}, C_{O_2}, L_o, A, T, \phi, V_s) \qquad (9)$$

where $C_{CO} = f(S_{CO})$, $T = f(C_{CO2})$, $\phi = f(C_{CO2})$, $C_{CO2} = f(V_s, A)$. Figure 5 shows that the electrical output, $L_o$, could be another independent factor in addition to $C_{CO2}$. It is reasonable to first consider only the dependence on $O_2$ level and output.

$$S_{CO} = f(C_{O_2}, L_O) \qquad (10)$$

The same approach can then be applied to the $O_2$ consumption rate.
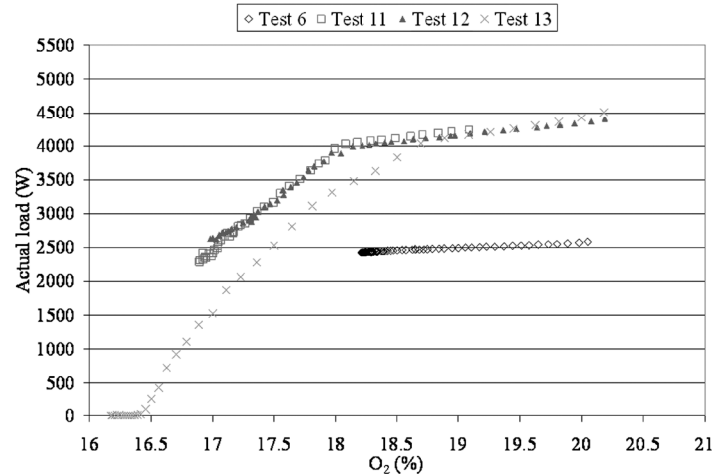
**Figure 5.** Measured generator real output loads of selected tests for different $O_2$ levels.

$$S_{O_2} = f(C_{O_2}, L_o) \qquad (11)$$

By using the noncommercial statistical analysis software package R,[13] nondimensional forms of eqs 10 and 11 were obtained as follows:

$$S^\star_{CO} = e^{-1.3504\,C^\star_{O_2} + 2.43738L^\star_o - 0.99583} - L^\star_o \qquad (12)$$

$$S^\star_{O_2} = e^{0.64191C^\star_{O_2} - 0.06588L^\star_o - 0.1939} - L^\star_o \qquad (13)$$

where the nondimensional parameter $S^\star_{CO}$ is defined by

$$S^\star_{CO} = \frac{S_{CO} - S_{CO,min}}{S_{CO,max} - S_{CO,min}} \qquad (14)$$

so that $0 \le S^\star_{CO} \le 1$. $S_{CO,min}$ and $S_{CO,max}$ are the minimum and maximum dimensional values of 5-min averaged CO generation rate, respectively. Similar definitions apply to the other nondimensional parameters $S_{O_2}$, $C_{O_2}$, and $L_o$. Table 3 provides the minimum and maximum values used to calculate the nondimensional values for correlation. Note that the correlations of eqs 12 and 13 may only apply to the specific generator tested in this study. Although other generators may share a similar form of correlations, the coefficients may be different.

Figure 6 compares the predicted CO generation and $O_2$ consumption rates using eqs 12 and 13 with those from the measurements. The predictions generally agreed well with the experiments except some data points (e.g.,

points 20 and 21 in Figure 6a). Note that the measured electrical output, $L_o$, was only available in tests 6, and 11–13 so that eqs 12 and 13 were obtained only using the measured data from these tests. The random discrepancies between prediction and measurement could potentially be reduced if more data points were used for correlation. However, eqs 12 and 13 show the potential to obtain correlations for CO generation and $O_2$ consumption rates for these types of experiments.

For an $O_2$ range of approximately 16–20.9% and an output load of approximately 0–5 kW, eqs 12 and 13 are plotted in Figure 7. Figure 7a shows that there seems be a point where the CO generation was minimal for each level of $O_2$. For example, when $O_2$ is at the ambient level, this condition exists when the generator is at half load. The $O_2$ consumption rates in Figure 7b look almost linear for each $O_2$ level because the coefficients of $C^\star_{O_2}$ and especially $L^\star_o$ in the exponential term of eq 13 are considerably smaller than in eq 12. On the basis of the limited range of data used to develop these correlations, the range of measured data is differentiated by shading it relative to the unshaded, extrapolated range in Figure 7.

## CONCLUSIONS

A series of experiments to measure CO generation from a portable, carbureted, spark-ignited, gasoline-powered electric generator without emission controls was conducted in a single-zone shed. It was found that the CO level in the shed reached a maximum value of 29,300 ± 580 mg/m³, whereas the $O_2$ was depleted to a minimum level of 16.2 ± 0.02% by volume. Under real weather conditions, CO generation and $O_2$ consumption could be expressed as time-averaged generation/consumption rates evaluated during the transient emission process. The rates of CO generation and $O_2$ consumption were affected by multiple parameters, with the $O_2$ level in the enclosed space and the actual electrical output of the generator being two of the most important. Correlations of CO generation and $O_2$ consumption rates with these two parameters were developed for this generator and found to agree well with experimental data. Although the results in this study may only apply to the specific generator
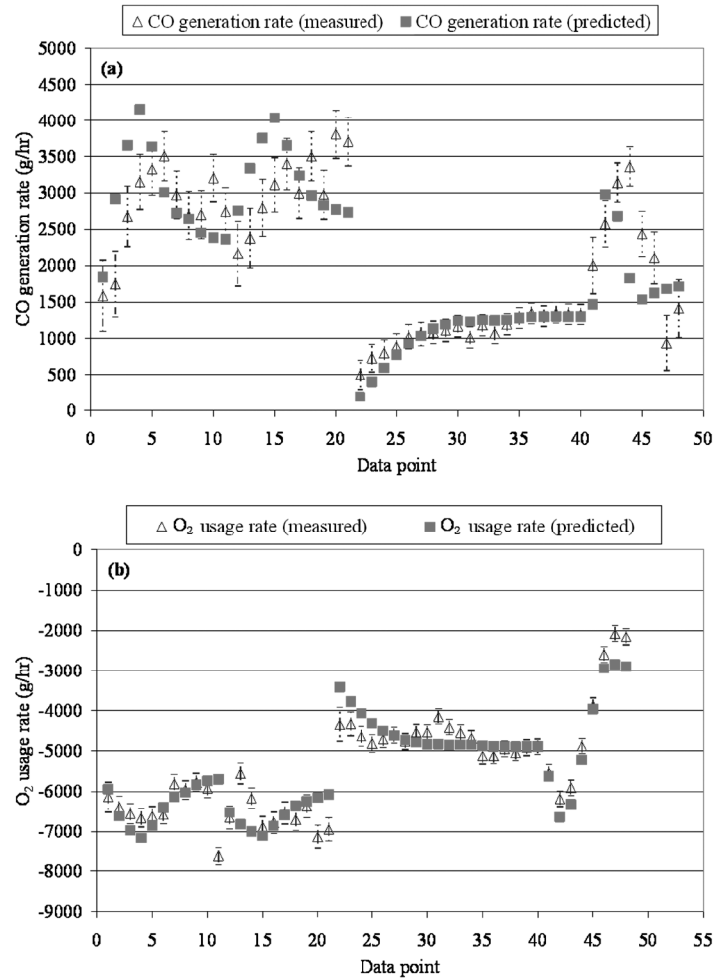
**Table 3.** Minimum and maximum values to calculate nondimensional parameters for the correlations of CO generation and $O_2$ consumption rates.

| 5-min Averaged Parameters | Minimum | Maximum |
|---|---|---|
| $S_{CO}$ (g/hr) | 500.0 | 4000.0 |
| $S_{O_2}$ (g/hr) | −7700 | −2050 |
| $C_{O_2}$ (%) | 16.0 | 20.9 |
| $L_o$ (kW) | 0.0 | 4300.0 |

**Figure 6.** Comparison of predicted (a) CO generation rates and (b) $O_2$ consumption rates with the measurement data.

tested, the experimental and analytical methods provided are important for additional studies of the indoor use of generators. The correlations developed in the study presented here will provide baseline CO emission rates for testing CO emission control devices. Further studies are needed to expand the correlations to other generators and to study CO migration and exposure in multizone residential houses.

**NOMENCLATURE**

$A_{in}$ = hourly air change rate of a test space evaluated at the ambient temperature, $hr^{-1}$

$A_{out}$ = hourly air change rate of a test space evaluated at the space temperature, $hr^{-1}$

$C_{CO}$ = CO concentration, $mg/m^3$

$C_{H2O,t1}$ = water vapor volumetric concentration at time $t_1$, $m^3/m^3$

$C_{H2O,t2}$ = water vapor volumetric concentration at time $t_2$, $m^3/m^3$

$C_{O2}^*$ = nondimensional $O_2$ concentration

$C_{out}$ = gas volumetric concentration outside of the space, $m^3/m^3$

$C_{SF6,in}$ = $SF_6$ concentration in the intake of the generator, $m^3/m^3$

$C_{SF6,ex}$ = $SF_6$ concentration in the exhaust of the generator, $m^3/m^3$

$D_{gen}$ = displacement of the generator engine, $m^3$

$K_{m,\rho}$ = $\rho_{m,out}/\rho_{m,in}$ = ratio of density outside and inside of the test space of a gas component, $m$

$K_{SF6,d}$ = $SF_6$ decomposition ratio in the generator

$L_o$ = output load of a generator

$L_o^*$ = nondimensional generator load

$P$ = partial pressure of water vapor, Pa

$P_{sat}$ = saturated water vapor pressure, Pa

$Q_{gen,in}$ = volumetric flow rate through the generator at the intake gas temperature, $m^3/hr$

$Q_{in}$ = volumetric air inflow of a test space, $m^3/hr$

$Q_{out}$ = volumetric air outflow of a test space, $m^3/hr$

$Q_{gen,ex}$ = volumetric flow rate through the generator at the exhaust gas temperature, $m^3/hr$

$RPM$ = revolutions per minute of the generator engine, $min^{-1}$

$S_C$ = source generation rate of a gas "C" at the air temperature of the test space, $kg/hr$

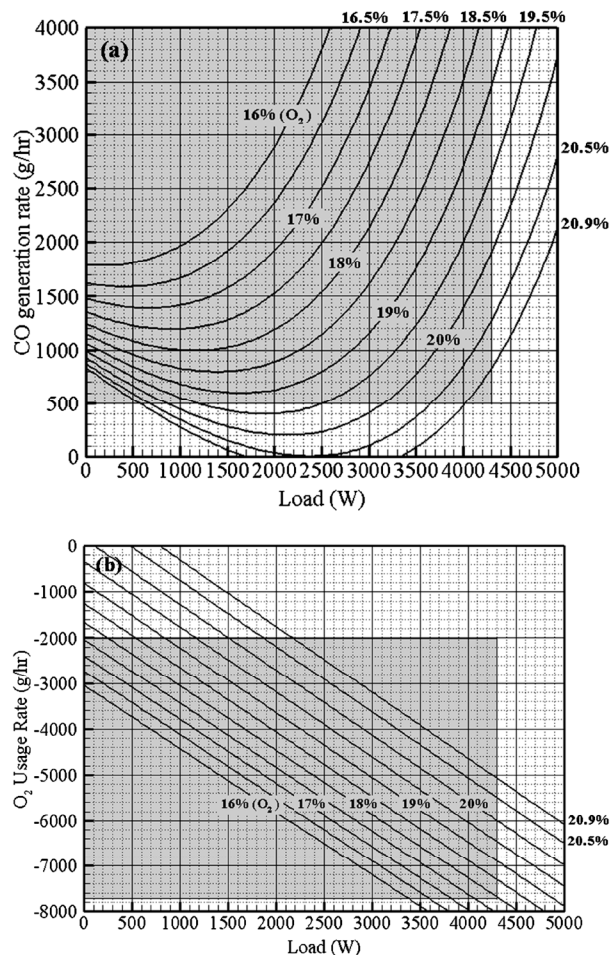$S_{CO}^*$ = nondimensional CO generation rate

**Figure 7.** Predicted (a) CO generation rate (g/hr) and (b) $O_2$ consumption rate (g/hr) as a function of generator output loads and $O_2$ levels (the shaded area is for the range of measurement data).

$S_{CO,min}$ = minimum CO generation rate, g/hr
$S_{CO,max}$ = maximum CO generation rate, g/hr
$S_{H2O}$ − water generation rate from the generator, kg/hr
$S_{gen}$ = mass added from the generator to the test space, kg/hr
$S_{O2}^*$ = nondimensional $O_2$ consumption rate
$T$ = temperature of the gas, K
$T_{gen,in}$ = temperature of the generator intake gas, K
$T_{gen,ex}$ = temperature of the generator exhaust gas, K
$V_s$ = volume of the test space, $m^3$
$\phi$ = water vapor relative humidity
$\eta_{gen}$ = volumetric efficiency of the generator engine
$\rho_{C,in}$ = density of a gas component inside of the test space, $kg/m^3$
$\rho_{C,out}$ = density of a gas component outside of the space, $kg/m^3$
$\rho_{in}$ = gas mixture density in the test space, $kg/m^3$
$\rho_{m,out}$ = density of gas mixture (= $\rho_{air}$) outside of the test space, $kg/m^3$
$\rho_{out}$ = ambient air density, $kg/m^3$

**REFERENCES**
1. Hnatov, M.V. *Incidents, Deaths, and In-Depth Investigations Associated with Non-Fire Carbon Monoxide from Engine-Driven Generators and Other Engine-Driven Tools, 1999–2007*; U.S. Consumer Product Safety Commission: Bethesda, MD, 2008; p 16.
2. *CPSC Portable Generators: Legal Memorandum and Staff Briefing Package for Advance Notice of Proposed Rulemaking (ANPR)*; U.S. Consumer Product Safety Commission: Bethesda, MD, 2006; p 295.
3. *CPSC Performance and Accountability Report*; U.S. Consumer Product Safety Commission: Bethesda, MD, 2007; p 140.
4. Stewart, R.D. The Effect of Carbon Monoxide on Humans; *Ann. Rev. Pharmacol.* **1975**, 15, 409-23.
5. Hnatov, M.V. *Non-Fire Carbon Monoxide Deaths Associated with the Use of Consumer Products 2003 and 2004 Annual Estimates*; U.S. Consumer Product Safety Commission: Bethesda, MD, 2007; p 21.
6. *Air Quality Criteria for Carbon Monoxide*; National Center for Environmental Assessment; Office of Research and Development; U.S. Environmental Protection Agency: Research Triangle Park, NC, 2000.
7. Kern, R.A.; Knoedler, J.A.; Trester, R.J. Automotive Carbon Monoxide Emissions in a Closed Garage. Presented at the International Congress and Exposition of Society of Automotive Engineers (SAE); SAE: Warrendale, PA, 1990; pp 33-38.
8. Brown, C.J. *Engine-Drive Tools, Phase 1 Test Report for Portable Electric Generators*; U.S. Consumer Product Safety Commission: Bethesda, MD, 2006; p 52.
9. *Material Safety Data Sheet (MSDS) for Sulfur Hexafluoride*; Airgas: Radnor, PA, 2006.
10. *Standard Test Method for Determining Air Change in a Single Zone by Means of a Tracer Gas Dilution*; American Society for Testing and Materials: West Conshohocken, PA, 2006.
11. Luce, C.; Heiser, B.; Siemer, M.; Smith, B. Redesign of the Mud Buggy to Reduce Emissions by Conversion to Propane Fuel. Presented at the Multi-Disciplinary Engineering Design Conference, Rochester, NY, 2006.
12. Proctor, C.L.; Berger, M.C.; Fournier, D.L.; Roychoudhury, S. *Sulfur Hexafluoride as a Tracer for the Verification of Waste-Destruction Levels in an Incineration Process: Final Report, May 1984–April 1986*; AD-A-181453/2/XAB; Department of Mechanical Engineering; University of Florida: Gainesville, FL, 1987.
13. Venables, W.N.; Smith, D.M.; The R Development Core Team. *An Introduction to R- Notes on R: A Programming Environment for Data Analysis and Graphics. Version 2.12.0.* R Foundation for Statistical Computing, Vienna, Austria, 2010. URL http://www.r-project.org/, ISBN 3-900051-12-7.

**About the Authors**
Liangzhu Wang is currently an assistant professor in the Department of Building, Civil, and Environmental Engineering at Concordia University in Montreal, Quebec, Canada. This research was conducted when he was a research associate at the Building and Fire Research Laboratory (BFRL) at NIST in Gaithersburg, MD. Steven J. Emmerich is a mechanical engineer in the BFRL at NIST, and Andrew K. Persily is the group leader of the Indoor Air Quality and Ventilation Group of the BFRL at NIST. Please address correspondence to: Steven J. Emmerich, 100 Bureau Drive, Stop 8633, Gaithersburg, MD 20899-8633; phone: +1-301-975-6459; fax: +1-301-975-4409; e-mail: semmerich@nist.gov.